Lysine methylation promotes NFAT5 activation upon EGFR activation and predicts the efficacy of temozolomide

Yuhong Wang
Tianjin Medical University
Yatian Li
Tianjin Medical University
Binbin Zhang
Tianjin Huanhu Hospital
Zhenyue Gao
Tianjin Medical University
Ruxin Hu
Tianjin Medical University
Yuqing Wang
Tianjin Medical University
Chao Liu
Tianjin Medical University Cancer Institute and Hospital
Xuebin Zhang
Tianjin Huanhu Neurological Hospital
Jingxuan Yang
The University of Oklahoma Health Sciences Center
Mei Mei
Tianjin Medical University
Yu Ren
Tianjin Medical University
Min Li (Min-Li@ouhsc.edu)
The University of Oklahoma Health Sciences Center https://orcid.org/0000-0002-3971-9130
Xuan Zhou

Article

Keywords: Lysine methylation, NFAT5, EZH2, EGFR activation, TMZ efficacy, GBM

Posted Date: May 2nd, 2022

DOI: https://doi.org/10.21203/rs.3.rs-950944/v1

Lysine methylation promotes NFAT5 activation upon EGFR activation and predicts the efficacy of temozolomide

Yuhong Wang[#,1], Yatian Li[#,1], Binbin Zhang[#,2], Zhenyue Gao[3], Ruxin Hu[3], Yuqing Wang[3], Chao Liu[4], Xuebin Zhang[5], Jingxuan Yang[6], Mei Mei[3], Yu Ren[1,*], Min Li[6,*] & Xuan Zhou[4,*]

[1]Department of genetics, School of Basic Medical Sciences, Tianjin Medical University, Tianjin, China; [2]Department of Neuro-oncology, Tianjin Huanhu Hospital, Tianjin, China; [3]Department of cell biology, School of Basic Medical Sciences, Tianjin Medical University, Tianjin, China; [4]Department of Maxillofacial and Otorhinolaryngology Oncology, Tianjin Medical University Cancer Institute & Hospital, Key Laboratory of Cancer Prevention and Therapy, Tianjin Cancer Institute, National Clinical Research Center of Cancer, Tianjin, China; [5]Department of Pathology, Tianjin Huanhu Hospital, Tianjin, China; [6]Department of Medicine, Department of Surgery, The University of Oklahoma Health Sciences Center, Oklahoma City, Oklahoma.

*email: xuanzhou@tmu.edu.cn; Min-Li@ouhsc.edu; yuren0925@tmu.edu.cn.

[#] These authors contributed equally.

Abstract

Temozolomide (TMZ) therapy exert limited clinical benefits in glioblastoma multiforme (GBM) patients with high EGFR activity, underscoring the need for effective combination therapy. Here, we show that tonicity-responsive enhancer binding protein (NFAT5) lysine methylation, is a determinant of TMZ response. Mechanistically, EGFR activation induces phosphorylated EZH2 (Ser21) binds to and triggers NFAT5 methylation at K668. Methylation prevents NFAT5 cytoplasm interaction with E3 ligase TRAF6, thus blocks TRAF6 induced K63-linked ubiquitination mediated NFAT5 lysosomal degradation and cytosol localization restriction, result in NFAT5 protein stabilization, nuclear accumulation and activation. Methylated NFAT5 leads to the upregulation of ITGB1, a transcriptional target of NFAT5, which is responsible for unfavorable TMZ response. Inhibition of NFAT5 K668 methylation improved TMZ efficacy in vivo. Notably, NFAT5 K668 methylation levels are elevated in TMZ-refractory specimens and confer poor prognosis. Our findings suggest targeting NFAT5 methylation as an effective therapeutic strategy to improve TMZ response in tumors with EGFR activation.

Keywords: Lysine methylation, NFAT5, EZH2, EGFR activation, TMZ efficacy, GBM

Introduction

Glioblastoma multiforme (GBM) is a highly aggressive cancer of the central nervous system, with a median survival time of only 12.2 months[1,2]. Temozolomide (TMZ), which is the mainstream chemotherapeutic agent for advanced GBM, offers a modest survival benefit of 14.6 months[3]. EGFR amplification and its constitutively active mutant, EGFRvIII (deletion of exons 2-7)[4], is a driving force in promoting GBM tumorigenesis and TMZ resistance[5-8]. However, the combination of anti-EGFR therapy with TMZ therapy yielded limited therapeutic benefits[9]. Therefore, it is critical to uncover the mechanisms underlying GBM pathogenesis and identify novel therapeutic targets to develop an efficacious combination therapy.

Tonicity-responsive enhancer binding protein (NFAT5, TonEBP), activated by hypertonicity, is initially identified as a central transcriptional regulator of osmoprotective response and the immune response[10,11]. Tonicity-regulated NFAT5 nuclear import depends on binding to the importin β1 (IMB1)[12]. Recent studies indicate that NFAT5 is overexpressed and associated with poor prognosis in GBM, pancreatic cancer, and melanoma[13-15]. Furthermore, NFAT5 regulates integrin-mediated cell adhesion and invasion[16]. As a key component of the integrin signaling pathway, integrin β1 (ITGB1) promotes TMZ resistance by suppressing p53 activity[17,18]. In particular, NFAT signaling was among the top two upregulated signaling pathways in TMZ treated U87/EGFRvIII expressing cells[19]. However, the regulatory mechanism governing NFAT5 activation independent on tonicity stimuli and its role in TMZ response remains elusive in GBM.

Lysine methylation of proteins is involved in subcellular localization, protein-protein interactions, and protein stability[20-22]. A series of studies reveal that histone methyl transferases such as EZH2 can modulate the signaling pathway activity through direct methylation of non-histone proteins[23-25]. Abnormal lysine methylation of non-histone proteins induced by growth factors such as EGF, leads to their hyperactivity and cancer progression[24,26,27]. Thus, targeting lysine methylation of non-histone protein can be potential therapeutic targets for cancer. However, whether and how lysine methylation regulates NFAT5 activity remain unknown.

In this study, we show that NFAT5 undergoes methylation at K668 by EZH2 upon EGFR activation. And we elucidate the underlying mechanism of the lysine methylation-dependent regulation of NFAT5 subcellular localization and function. Furthermore, we identify a role for NFAT5 K668 methylation in modulating the response to TMZ via up-regulation of *ITGB1* transcription both in vitro and in vivo. High levels of NFAT5 K668 methylation is associated EGFR activity, TMZ refractory and poor survival in GBM. These findings suggest that targeting NFAT5 methylation could be a novel therapeutic strategy to enhance the TMZ response in patients with GBM exhibiting upregulated EGFR activity.

Results

NFAT5 expression is up-regulated in TMZ-resistant GBM specimens and positively correlates with p-EGFR expression

To determine the clinical significance of NFAT5, immunohistochemistry (IHC) analysis was performed to examine the NFAT5 levels in 83 glioma specimens and adjacent non-tumor brain (NB) tissues obtained from the Tianjin Huanhu Hospital. We found significantly elevated NFAT5 expression in GBM tissue compared with those in low-grade gliomas (LGGs) and adjacent NBs ($P < 0.0001$; **Fig. 1a and Supplementary Table 1)**. Moreover, IHC scores revealed that 69.1% of (38/55) GBM samples display elevated NFAT5 expression. While the median survival durations of glioma patients harboring tumors with low and high NFAT5 expression was19.9 and 9.8 months ($P = 0.009$; **Fig. 1b**). The median survival durations of GBM patients harboring tumors with low and high NFAT5 expression was 17.8 and 8.9 months, respectively ($P = 0.038$; **Supplementary Fig. 1a**). These data suggest NFAT5 overexpression may contribute to GBM progression.

Aberrant EGFR activation contributes to GBM progression and TMZ resistance development[28]. To examine the relationship between EGFR activity and NFAT5 levels in the clinical setting, the expression of EGFR pY1068 and NFAT5 were analyzed in the 83 glioma specimens **(Fig. 1c)**. In particular, 63.3% of (31/49) tumor samples with high NFAT5 expression exhibited a strong p-EGFR staining. Meanwhile, 66.7% of (10/15) samples with low NFAT5 expression had weak or no p-EGFR IHC signal. The expression of NFAT5 in GBM tissues was upregulated compared with adjacent NBs and positively correlated with that of p-EGFR **(Fig. 1d)**. These results indicate that NFAT5 expression is physiologically and clinically relevant to EGFR activity in GBM.

Moreover, the expression and nuclear localization of NFAT5 were higher in TMZ-refractory samples than those in TMZ-sensitive specimens **(Fig. 1e, f)**. Collectively, these results show that NFAT5 expression, which is correlated with EGFR activity, and is upregulated in TMZ-refractory tissues.

NFAT5 is required for EGFR driven tumor growth and the failure of TMZ therapy

To explore the function of NFAT5 in regulating cancer drug resistance, we first obtained the TMZ response data across 505 cancer cell lines from the Genomics of Drug Sensitivity in Cancer (GDSC) database (https://www.cancerrxgene.org/). NFAT5 expression displayed significant association with the resistance to TMZ, especially in GBM cell lines (P = 0.017; **Fig. 2a, Supplementary Fig. 1b).** We next examined the expression of NFAT5 in various GBM cell lines. NFAT5 expression in TMZ resistant (U87/EGFRvIII cells) was significantly upregulated compared with that in TMZ sensitive cells (U251, U87, and LN229 cells) (**Supplementary Fig. 1c**). To study the role of NFAT5 in regulating TMZ sensitivity, we first constructed NFAT5-overexpressing and knockout stable cell lines (**Supplementary Fig. 1d-g**). The half-maximal inhibitory concentration (IC_{50}) value of TMZ against NFAT5-overexpressing U87/EGFR and U251 cells increased by 4.04- and 2.87-fold, respectively **(Fig. 2b)**. In contrast, loss of NFAT5 markedly enhanced the TMZ sensitivity in U87/EGFRvIII cells **(Fig. 2c).** Consistently, in vitro colony formation ability was reduced and the percentage of apoptotic cells were significantly increased in TMZ treated NFAT5 deficiency U87/EGFRvIII cells (**Fig. 2d, e and Supplementary Fig. 1h**). NFAT5 knockdown inhibited cell proliferation and TMZ resistance in U87/EGFRvIII cells (**Fig. 2f).** Moreover, knockdown of NFAT5 inhibited EGF stimulation induced cell proliferation and TMZ resistance in U251 and U87/EGFR cells (**Fig. 2g).**

Next, the role of NFAT5 in regulating the efficacy of TMZ *in vivo* was assessed. TMZ therapy exerted a limited tumor-inhibitory effects against sg-NC-transfected U87/EGFRvIII cells. Bioluminescent images and hematoxylin and eosin (H&E) staining shown that the loss of NFAT5 significantly abrogated EGFR driven tumor growth and enhanced the sensitivity of tumors to TMZ **(Fig. 2h, i)**. Additionally, the survival time of TMZ treated mice harboring tumors with sg-NFAT5 transfected cells was higher than that of mice belonging to other groups **(Fig. 2j)**. Therefore, NFAT5 is required for EGFR activation-induced tumor growth and limited TMZ efficacy.

EGF induces NFAT5 lysine methylation and activation dependent on EZH2

As EGFR activation is critical for tumorigenesis and TMZ resistance, the effect of EGF

stimulation on NFAT5 expression and activation was examined in multiple GBM cells. Western blotting analysis revealed NFAT5 protein levels were upregulated in U87/EGFR and U251 cells upon EGF stimulation (**Fig. 3a**). No significant increase of NFAT5 mRNA was observed in U251 and U87/EGFR cells upon EGF stimulation (**Supplementary Fig. 2a**). Western blotting and immunofluorescent staining revealed enhanced nuclear abundance of NFAT5 in EGF-treated U87/EGFR cells (**Fig.3b and Supplementary Fig. 2b)**. A higher amount of nuclear NFAT5 levels were observed in the EGFR-constitutively active U87/EGFRvIII cells than in U87/EGFR cells **(Fig.3b and Supplementary Fig. 2c)**. Additionally, EGF stimulation increased NFAT5 protein stability (**Supplementary Fig. 2d**). These results indicate that EGF regulates NFAT5 expression through post-translational modification.

Methylation of lysine residues affect subcellular localization and protein stability[29,30]. As shown in **Fig.3c**, EGF stimulation induced NFAT5 lysine tri-methylation (Me^3 K) but not mono or demethylation ($Me^{1,2}$ K) in U87/EGFR cells in a time-dependent manner. To explore the downstream pathway involved in NFAT5 methylation in response to EGF stimuli, cells were treated with several small-molecule inhibitors of the EGFR downstream pathway, including perifosine (AKT1 inhibitor), U0126 (MEK1 inhibitor), and GF109203X (PKCα inhibitor), respectively. Treatment with perifosine markedly blocked EGF-induced NFAT5 methylation **(Fig. 3d and Supplementary Fig. 2e)**. Consistently, knockdown of AKT1 by shRNA mitigated NFAT5 methylation induced by EGF (**Supplementary Fig. 2f**). The levels of NFAT5 methylation in the AKT1 kinase-dead K179M mutant-transfected cells was markedly lower than that in the AKT1 WT-transfected cells, suggesting that AKT1 kinase activity was required for EGF-mediated NFAT5 methylation (**Fig. 3e**).

Previous studies reported that Ser21 of EZH2 is a substrate of AKT1[31]. Phosphorylation of EZH2 at Ser 21 exerts pro-tumorigenic functions in a non-histone methylation-dependent manner in several types of cancer[25,32]. An in vitro phosphorylation assays using constitutively active E40K mutant and kinase-dead mutant K179M confirmed that AKT1-mediated EZH2 phosphorylation at Ser21 (**Fig. 3f**). EZH2 knockdown by shRNA or treatment with DZNep (a small molecule inhibitor of EZH2), largely reduced EGF-

induced NFAT5 lysine methylation **(Fig. 3g and Supplementary Fig. 2g)**. The results of Co-IP and proximity ligation assays (PLA) confirmed that NFAT5 physical interacted with EZH2 in U251 cells (**Fig. 3h, i**). EGF induced NFAT5 methylation and the association with EZH2 in EZH2 WT but not S21A mutation (**Fig. 3j**). Furthermore, NFAT5 methylation was detected in the EZH2 S21D expressing cells similar as EGF treated EZH2 WT cells (**Supplementary Fig. 2h**). Additionally, the H3K27me^3 enrichment in the promoter region of NFAT5 was not affected in EZH2 knockdown treated cells (**Supplementary Fig. 2i**). These results suggest that EZH2 is the critical methyltransferase for NFAT5 lysine methylation upon EGFR activation.

We next investigated the role of lysine methylation on NFAT5 protein stability and activation. Western blotting and immunofluorescent staining revealed that knockdown EZH2 reduced EGF induced NFAT5 nuclear translocation, whereas expression of EZH2 WT, but not S21A rescues NFAT5 nuclear distribution resulting from EZH2 knockdown (**Fig. 3k and Supplementary Fig. 3a)**. We then used an EZH2 mutant in which the NLS motif was deleted and fails to enter the nucleus, this mutation inhibited the nucleation of NFAT5 mediated by EGF, so we speculate that the nucleation of EZH2 was the key factor for NFAT5 to enter the nucleus (**Supplementary Fig. 3b and c**). Loss of EZH2 reduced NFAT5 transcriptional activity, which was restored by the EZH2-WT, but not S21A mutant groups, suggesting that phosphorylation of EZH2 at S21 was required for NFAT5 activity (**Fig. 3l**). Moreover, knockdown of EZH2 obviously decreased NFAT5 protein stability and half-life time (**Fig. 3m**).

Collectively, these findings imply that EZH2 is required for NFAT5 lysine methylation and activation in response to EGF stimulation.

Methylation at K668 determines NFAT5 nuclear localization and activation

We explored mass spectrometry analysis to identify the specific methylation sites of NFAT5. Two lysine residues (K616 and K668), which were located in the C-terminal transactivation domain (TAD), were identified in NFAT5 (**Fig. 4a and Supplementary Fig. 4a**). Moreover, both residues were highly conserved from Gallus Gallus to humans (**Supplementary Fig. 4b**). The methylation status of NFAT5 K668R mutant, but not the

K616R mutant, was significantly lower than those of NFAT5 WT upon EGF stimulation (**Fig. 4b**). In contrast to NFAT5 WT, K668R mutants was disassociated with EZH2.

Next, a K668-specific methylation antibody against NFAT5 was generated to identify K668 tri-methylation of NFAT5 (anti-Me^3-NFAT5 K668), which was validated by dot blot, ELISA and IF staining (**Supplementary Fig. 4c-e**). Analysis with pan-lysine tri-methylation and anti-Me^3-NFAT5 K668 revealed that EGF induced NFAT5 K668 tri-methylation in NFAT5 WT cells, which was mitigated in NFAT5 K668R overexpressing cells (**Supplementary Fig. 4f**). Additionally, NFAT5 K668 methylation was impaired in cells infected with shEZH2 or DZNep treatment (**Fig. 4c and Supplementary Fig. 4g**). Of note, the NFAT5 K668 tri-methylation in EZH2 WT but not S21A was markedly enhanced in response to EGF stimulation. Expression of constitutively active EZH2 S21D mutant was sufficient to induce NFAT5 K668 methylation to a degree similar to that observed in response to EGF treatment (**Fig. 4d**). Meanwhile, elevated NFAT5 K668 methylation levels were observed in the EGFR-constitutively active U87/EGFRvIII cells, compared to EGF treated U87/EGFR cells (**Supplementary Fig. 4h**).

We then sought to examine whether K668 methylation influence NFAT5 localization. Biochemical fractionations/western blot analysis and immunofluorescence revealed that EGF treatment induced the nuclear accumulation of NFAT5 WT but not K668R mutant expressing cells (**Fig. 4e, f and Supplementary Fig. 5a**). NFAT5 K668 methylation was detected in the cytosol peaked at 5min in response to EGF treatment, and was recruited to the nucleus (**Supplementary Fig. 5b**). These results indicate that EZH2-mediated NFAT5 methylation at K668 is likely to initially occurred in the cytosol, and is crucial for NFAT5 nuclear accumulation upon EGF stimulation.

Recent studies have shown that IMB1, a nuclear transport receptor, is required for NFAT5 nucleus translocation[12]. Co-IP confirmed that NFAT5 interacted with IMB1 in U251 cells (**Fig. 4g**). As expected, EGF stimulation increased the binding of NFAT5 and IMB1, while the interaction was greatly weakened in NFAT5 K668R mutant cells (**Fig. 4h**). Consistently, knockdown IMB1 reduced EZH2 induced the NFAT5 nuclear accumulation (**Fig. 4i and Supplementary Fig. 5c**). Meanwhile, EZH2 S21A reduced the binding of

NFAT5 and IMB1, compared to EZH2 WT cells (**Supplementary Fig. 5d**). Notably, NFAT5 K668R mutant showed decreased transcriptional activity (**Fig. 4j**). These results suggest that methylation at K668 promotes NFAT5 binding to IMB1, result in NFAT5 nuclear localization and activation upon EGFR activation.

Methylation protects NFAT5 from ubiquitin-mediated lysosome degradation by attenuating its binding to E3 ligase TRAF6

As expected, K668R mutant reduced NFAT5 protein stability and half-life time **(Fig. 5a)**. Meanwhile, the degradation of NFAT5 K668R was inhibited by concanamycin-A (ConA, an inhibitor of lysosome), but not MG132 (an inhibitor of proteasome) or 3-Methyladenine (3-MA, an inhibitor of autophagy) treatment **(Supplementary Fig. 6a)**. NFAT5 K668R mutant increased the association between NFAT5 with LAMP2 (**Fig.5c)**. Consistently, the NFAT5/LAMP2 complex formation was enhanced by shEZH2 transfected or DZNep treated cells **(Supplementary Fig. 6b)**. Immunofluorescence showed that NFAT5 K668R mutant increased the co-localization of NFAT5 and LAMP2 **(Supplementary Fig. 6c)**.

Lysine methylation modulates protein stability through regulating ubiquitination modification[33,34]. K668R mutant obviously increased the ubiquitination of NFAT5 (**Supplementary Fig. 6f**). Similar results were detected in cells knockdown EZH2 with shRNA or DZNep treatment (**Supplementary Fig. 6d, e**). Furthermore, EGF reduced K63- but not K48-linked ubiquitination of NFAT5, whereas such ubiquitination was markedly induced in K668R mutant expressing cells **(Fig. 5b and Supplementary Fig. 6g, h)**. We further demonstrated that the K63-linked ubiquitination of NFAT5 was observed only in the cytosol (**Supplementary Fig. 6i**). These results show that K668 methylation of NFAT5 increases protein stability by inhibiting K63-linked ubiquitin-mediated lysosomal degradation in the cytoplasm.

The ubiquitin dependent lysosomal degradation requires the endosomal sorting complexes required for transport (ESCRT) complexes, including HRS, STAM1 and STAM2[35]. Co-IP results indicated that the association of NFAT5 with STAM1, but not HRS nor STAM2, was decreased in NFAT5 K668R cells compared with NFAT5 WT cells **(Fig. 5c)**. Furthermore, knockdown of STAM1 rescued NFAT5 degradation induced by

methylation blockade (**Supplemental figure 6j**), further confirming the requirement of the ESCRT-0 complex in lysine methylation-induced NFAT5 stabilization.

To identify the putative E3 ligases that catalyzed NFAT5 K63-linked ubiquitination, liquid chromatography-tandem mass spectrometry/mass spectrometry (LC-MS/MS) analysis was performed and TRAF6 was revealed as a potential E3 ligases of NFAT5 (**Supplementary Fig. 7a**). The results of co-IP confirmed that NFAT5 physical interacted with TRAF6 in U251 cells **(Fig. 5d)**. TRAF6 significantly promotes the K63 but not K48-linked ubiquitination of NFAT5. On the contrast, mutation of TRAF6 in the RING domain ($TRAF6^{C70A}$), which was required for E3 ligase activity, lose the ability to ubiquitinate NFAT5 **(Fig. 5e)**. Moreover, TRAF6 mediated cytoplasmic K63-linked ubiquitination of NFAT5 in U251 cells (**Supplementary Fig. 7b**). These results suggest that TRAF6 is a K63 specific ubiquitin ligase for NFAT5. Moreover, the association between NFAT5 and TRAF6 was markedly increased in NFAT5 K668R cells upon EGF stimulation, compared to the NFAT5 WT cells. IF staining showed that the localization signal of NFAT5 and TRAF6 was seen by yellow staining in most of NFAT5 K668R mutant cells, but not NFAT5-WT cells **(Supplementary Fig. 7c)**. Meanwhile, knockdown TRAF6 could restore NFAT5 expression in NFAT5 K668R mutant or shEZH2 cells **(Supplementary Fig. 7d, e)**.

Therefore, these data indicate that K668 methylation of NFAT5 is a critical signal to mask the recognition of E3 ligase TRAF6 to NFAT5, consequently protecting NFAT5 from ubiquitin-mediated lysosome degradation.

NFAT5 K668 methylation interferes TRAF6 induced NFAT5 cytosol localization restriction

TRAF6 mediated ubiquitination is also involved in protein subcellular distribution[36,37]. IF staining combined with biochemical fractionations/western blot results demonstrated that knockdown of TRAF6 enhanced the nuclear localization of NFAT5 in the absence of EGF stimulation (**Fig. 5f and Supplementary Fig. 7f**). To elucidate the mechanism by which TRAF6 controls NFAT5 nuclear distribution, we determined whether TRAF6 mediated NFAT5 K63-linked ubiquitination orchestrates the interaction between NFAT5 with IMB1. Overexpressing TRAF6 blocked the association of NFAT5 and IMB1 in the

absence of EGF treatment. And the binding affinity of NFAT5 to IMB1 was restored upon EGF stimulation in NFAT5 WT cells, but not in K668R mutant expressing cells (**Fig. 5g**). Immunofluorescence staining confirmed that knockdown of TRAF6 significantly increased the co-localization signal of NFAT5 and IMB1 **(Fig. 5f)**. NFAT5 interacted with TRAF6 at serum starved condition, and then declined rapidly with the prolongation of EGF treatment. On the contrary, EGF stimulation induced the binding of NFA5 to EZH2 and IMB1 (**Supplementary Fig. 7g**). NFAT5 K668R mutant displayed strong association of TRAF6 and marked reduction in interacting with EZH2 and IMB1 under basal conditions and or EGF treatment. Consistently, TRAF6 induced the association of NFAT5 with LAMP2 and STAM1 in control cells, which was significantly reduced in EZH2 overexpressing cells **(Fig. 5h).** These results suggested that TRAF6 induced NFAT5 cytosol localization restriction through disrupting the interaction between NFAT5 and IMB1.

To underlying the mechanism involved in NFAT5 K668 methylation reduced the binding affinity of TRAF6, we constructed fragmented plasmids of different domains of NFAT5. Result of Co-IP showed that both N2 and N4 domain were the critical domain for NFAT5 and EZH2 as well as IMB1 binding. TRAF6 bounds to NFAT5 at the N1 and N4 domain **(Fig. 5i)**. N1 domain and N2 domain are reported to modulate NFAT5 nuclear export and import, respectively. N4 domain, where K668 site was located, was critical for NFAT5 activation[38]. These results indicate that EZH2-induced NFAT5 methylation disrupts the interaction between NFAT5 and TRAF6, leading to NFAT5 binding to IMB1 and translocating to the nucleus.

These results suggest that TRAF6 triggers NFAT5 ubiquitination reduces the interaction between NFAT5 and IMB1, thus keeping NFAT5 away from the nucleus. NFAT5 K668 methylation by EZH2 disrupts the association with TRAF6 and NFAT5, leading to NFAT5 nuclear translocation.

K668 methylation is required for NFAT5 induced limited TMZ efficacy by enhanced *ITGB1* transcription

To unveil the significance of NFAT5 K668 methylation in modulating the efficacy of TMZ therapy, the growth-inhibitory efficacy of TMZ against NFAT5 WT and K668R mutant-

transfected cells was examined. The IC_{50} of TMZ in NFAT5-K668R cells was 2.45- and 3.31-fold lower than those against NFAT5 WT transfected U251 and U87/EGFR cells, respectively **(Fig. 6a)**. Additionally, in vitro colony formation ability in the TMZ treated NFAT5 K668R expressing cells were largely reduced, compared to NFAT5 WT cells **(Fig. 6b).**

To identify the downstream gene of NFAT5 in modulating TMZ efficacy, mRNA sequencing was performed to analyze the signaling pathways associated with NFAT5 upregulation. Differentially expressed genes (DEGs) were enriched in “Apoptosis” and “ECM-receptor interaction” pathways based on the Kyoto Encyclopedia of Genes and Genomes (KEGG) pathway analysis **(Supplementary Fig. 8a)**. The integrin signaling pathway was reported to be critical for tumor progression, metastasis, and TMZ resistance therapy in GBM[17,39]. Hence, the regulatory effect of NFAT5 on the key members of the integrin signaling pathway in GBM cells was examined. NFAT5 overexpression increased mRNA and protein levels of *ITGB1*, whereas NFAT5 deficiency reduced *ITGB1* expression **(Fig. 6c and Supplementary Fig. 8b)**. However, NFAT5 did not affect the levels of *ITGB3* or *ITGB6* **(Supplementary Fig. 8c)**.

ITGB1 is reported to induce TMZ resistance by suppressing p53 activity[17]. Next, the regulatory effects of NFAT5 on TMZ resistance through *ITGB1* were examined. The expression of *ITGB1* was stably knocked down in NFAT5-overexpressing cells **(Supplementary Fig. 8d**). The IC_{50} of TMZ against *ITGB1* knockdown U87/EGFR and U251 cells overexpressing NFAT5 decreased by 4.38- and 2.54-fold, respectively **(Fig. 6d).** Overexpression of NFAT5 inhibited TMZ-induced p53 expression, whereas knockdown ITGB1 rescues the p53 activity resulting from NFAT5 overexpression **(Supplementary Fig. 8e)**.

To uncover the mechanism of NFAT5-induced ITGB1 transcription, the potential binding sites of NFAT5 in the promoter region of *ITGB1* were searched in the HumanTFDB database and three putative binding sites were identified. The luciferase reporter plasmid carried the putative binding site of NFAT5 to ITGB1 promoter was constructed. Luciferase activity was significantly increased in NFAT5 overexpressing cells. As shown in **Fig.6e**, the

binding motif-3 was required for NFAT5-induced *ITGB1* transcription. These data reveal that ITGB1 is a direct transcriptional target of NFAT5.

ChIP-PCR data showed that NFAT5 K668R mutation significantly reduced the binding of NFAT5 to the promoter of *ITGB1* (**Fig. 6f**). Consistently, EGF increased the binding of NFAT5 to the promoter of *ITGB1*, whereas the absence of EZH2 reversed this effect **(Fig. 6g, h and Supplementary Fig. 8f, g)**. In contrast to NFAT5 WT, NFAT5 K668R mutant transfection cells didn't upregulate the mRNA nor protein levels of *ITGB1* (**Fig. 6i and Supplementary Fig. 8h).**

Collectively, these results suggest that NFAT5 K668 methylation attenuates TMZ efficacy by enhancing the transcription of *ITGB1*.

Inhibition of NFAT5 K668 methylation improves TMZ efficacy in vivo

To examine the role of NFAT5 K668 methylation in conferring TMZ efficacy *in vivo*, NFAT5 WT or K668R mutant was stably overexpressed in U87/EGFRvIII cells. Bioluminescence and H&E staining analyses revealed that the growth of NFAT5 K668R-transfected cell-derived tumors was slower than that of NFAT5 WT cell-derived tumors. (**Fig. 7a and Supplementary Fig. 9a**). Meanwhile, the NFAT5 K668R mutant prolonged survival time, compared with NFAT5 WT group mice (**Fig. 7b**). Reduced Ki67 and elevated cleaved caspase-3 expression were detected in TMZ treated NFAT5 K668R cell-derived tumors (**Supplementary Fig. 9b, c**). This indicates that NFAT5 K668R cells exhibited increased sensitivity to TMZ.

To further validate these findings in vivo, an orthotopic to GBM tumor model derived by U87/EGFRvIII cells was employed to test the anti-tumor effect of DZNep/TMZ combined regimen. The combination therapy reduced the tumor size and prolonged survival time, compared to the single TMZ-treated mice (**Fig. 7c-e**). Moreover, tumors with combination therapy largely reduced Me^3-NFAT5 K668 levels and the association between NFAT5 and EZH2 or TRAF6, compared with TMZ-treated mice (**Fig. 7f, g**). Meanwhile, increased cleaved caspase3 and reduced Ki67 signals were detected in DZNep/TMZ combination treatment group **(Supplementary Fig. 9d, e)**

These results indicate that Me^3-NFAT5 K668 is a master regulator of tumor progression and TMZ response, and may serve as a potential therapeutic target for patients with GBM exhibiting enhanced EGFR activity.

NFAT5 K668 methylation is positively correlated with p-EGFR Y1086 and p-EZH2 S21 expression, TMZ refractory and poor prognosis in patients with GBM

To determine the clinical significance of EGFR/EZH2 dependent NFAT5 lysine methylation in glioma, we performed IHC analysis to examine the expression and correlation between EZH2 pS21 and Me^3-NFAT5 K668 as well as EGFR pY1068 levels in 83 human glioma specimens. A total of 57.1% (32/56) glioma specimens with high NFAT5 K668 methylation levels displayed enhanced protein expression of EZH2 pS21. Meanwhile, 62.5% (35/56) glioma specimen with high NFAT5 K668 methylation levels displayed enhanced protein expression of EGFR pY1068 (**Fig. 8a**). These findings suggest that the expression of Me^3-NFAT5 K668 is positively correlated with EGFR pY1068 and EZH2 pS21 in glioma ($P < 0.0001$; **Fig. 8b**).

Next, we found elevated Me^3-NFAT5 K668 expression and nuclear abundance in TMZ-resistant, compared with sensitive GBM specimens **(Fig. 8c, d)**. To further determine the clinical relevance of Me^3-NFAT5 K668 level to the prognosis of GBM patients, we analyzed Me^3-NFAT5 K668 levels and survival duration. The medium survival of the GBM patient with low Me^3-NFAT5 K668 levels is 36 months, while the medium survival is 12 months in high-Me^3-NFAT5 K668 GBM patients (**Fig. 8e**). This indicates that NFAT5 K668 methylation level is a robust and independent predictor of survival for patient with GBM.

Discussion

Unfavorable TMZ response remains the leading challenge for in GBM patients with aberrant EGFR activation[5,40]. This study uncovered that lysine methylated NFAT5, an osmoprotective responsive transcription factor, is a determinant of EGFR driven tumor progression and the response to TMZ in GBM, reinforcing the key role of lysine methylation of non-histone proteins and demonstrating its potential as a novel source of therapeutic targets. We found that EGFR activation orchestrated sequential PTM events involving lysine methylation and ubiquitination to control NFAT5 nuclear localization and activation.

The main mechanisms of TMZ drug resistance are MGMT overexpression or DNA repair deficiency[41,42]. To our knowledge, this is the first report on the function of NFAT5 in chemoresistance in GBM. EGFR activation supports NFAT5 interaction with EZH2 and triggers NFAT5 methylation at K668. Methylation result in NFAT5 stabilization, nuclear accumulation and activation. In particular, we reveal that methylated NFAT5 is involved in the transcriptional upregulation of *ITGB1*, which are crucial effectors for TMZ-mediated cytotoxicity (**Fig. 8f**). These results clearly support the notion that the previously uncharacterized EGFR/EZH2/NFAT5 axis identified may explain the high probability of tumorigenesis and why only a small fraction of GBM patients respond to TMZ. The abundant K668 methylation of NFAT5 was elevated in TMZ resistant GBM specimens. Moreover, increased levels of NFAT5 K668 methylation was correlated with EGFR activity and conferred poor prognosis in patient with GBM. Thus, this study provides clinical and mechanistic evidence demonstrating that NFAT5 methylation is critical for EGFR-driven tumorigenesis and poor TMZ efficacy in GBM.

NFAT5 regulates the osmotic pressure balance through regulating multiple downstream genes[11]. However, the mechanism underlying the regulation of NFAT5 nuclear translocation and protein stability during cancer progression, especially upon growth factor stimulation, remains unclear. We identify TRAF6 E3 ligase as a critical cytosolic gatekeeper to keep NFAT5 away from nucleus and routed to lysosomal degradation under the serum starved condition. Mechanistically, we show that TRAF6 interacts with cytosolic NFAT5 and triggers K63-linked ubiquitination of NFAT5, which prevents NFAT5 from binding to IMB1,

consequently restrict NFAT5 cytosol localization. Moreover, TRAF6 induced NFAT5 polyubiquitination, thereby inducing its association with the core components of the ESCRT-0 complex STAM1 and facilitated NFAT5 lysosome mediated degradation. EZH2 binds to the NFAT5 in a competitive manner with TRAF6 upon EGF stimulation. Therefore, NFAT5 K668 methylation serves a molecular switch that regulates NFAT5 nucleus translocation and stability in GBM in response to EGFR activation.

EZH2 is mainly reported to function as a histone methyltransferase through its SET domain[43,44]. EZH2 as a methyltransferase modulates Erα and PP2A that are associated with targeted therapy resistance, which modulating tamoxifen resistance in breast cancer[45,46]. Our findings identify NFAT5 as a novel non-histone substrate of EZH2. We found a positive correlation between the protein expression of p-EZH2 S21 and NFAT5 K668 methylation in GBM specimens. We expand the understanding of EZH2 substrates and its biological function. Therefore, the elucidation of the effect of non-histone lysine methylation on chemo-resistance might contribute to clinical application to improve the survival of patient with GBM.

In summary, we showed that NFAT5 K668 methylation is a key event regulating NFAT5 hyperactivation and the response of TMZ therapy. These findings provide a rationale for targeting NFAT5 K668 methylation combined with TMZ therapy for GBM patients with abnormal EGFR activation.

Methods

Patient samples

A total of 83 glioma tissue specimens were collected from the Tianjin Huanhu Hospital. All patients voluntarily signed an informed consent form. This study was approved by the Tianjin Huanhu Hospital Ethical Committee (EK 2019179). The clinical stage of the tumor was determined and matched to the gender and age according to the American Joint Committee on Cancer (8^{th} edition) guidelines. The response to TMZ therapy was evaluated according to the Response Evaluation Criteria for Solid Tumors 1.1. Patients with complete or partial response were defined as "sensitive," whereas those who exhibited tumor progression or stable were defined as “resistant.”

Cell lines and reagents

Human GBM cell lines (U87, U251, and LN229 cells) were purchased from the American Type Culture Collection (ATCC). The U87/EGFRvIII cell line was a kind gift from Prof. Han (Tianjin Medical University General Hospital, Tianjin, China)[47]. LN229, U251, and U87/EGFRVIII cells were cultured with Dulbecco's modified Eagle medium, and U87 cells were cultured with Eagle’s minimum essential medium. The culture medium was supplemented with 100 U/mL penicillin, 100 μg/mL streptomycin, and 10% fetal bovine serum. The cells were cultured at 5% CO_2 and 37°C. Only cells cultured to the log phase and passaged ≤ 15 times were used.

TMZ (T-36587), DZNep (S7120), GF109203X (S7208), and U0126 (S1102) were purchased from Selleck Chemicals. EGF was acquired from Sino Biological (10605-HNAE).

Generation of stable cells using lentiviral transfection

To establish the human *NFAT5* knockout cells, the cells were transfected with lentiviral vectors harboring clustered regularly interspaced short palindromic repeats/caspase 9 sequences targeting human *NFAT5*. The target sequences were as follows: sgNFAT5 #1, 5′-CAGCTTACCACGGACAACAA-3′; sgNFAT5 #2, 5′-GGATATTGTCCACACAACAT-3′; and sgNFAT5 #3, 5′-GCGTAGGGATATTGAAATTG-3'. The cells were seeded at 50% confluency 24-36 h before lentiviral transfection. After transfection for 16h, the medium was

removed and cells were cultured in medium containing 4μg/mL puromycin after 16 h of transfection for one week.

To generate the cells expressing NFAT5 wild-type (WT) or K668R mutant, the lentiviral vectors harboring Flag-tagged WT or K668R mutant NFAT5 sequences, which were purchased from Genechem (China), were transfected into sgNFAT5-transfected cells. The cells were seeded at 50% confluency 24-36 h before infection. The medium was replaced with a medium containing lentiviral vectors. After transduction for 16 h, the medium was replaced with fresh medium and the transfected cells were selected with 600 μg/mL G418 (Sigma) for 2 weeks.

To establish stable *EZH2* knockdown lines, the cells were transfected with a lentiviral short hairpin RNA (shRNA) system (Genechem) containing the following shRNA against *EZH2* (shEZH2): 5'-CCGGCCCAACATAGATGGACCAAATCTCGAGATTTGGT CCATCTATGTTGGGTTTTTG-3'. The target sequences used for shITGB1 were as follows: shITGB1 #1, 5′-GGCUCCAAAGAUAUAAAGATT-3′; shITGB1 #2, 5′-GCCUUCAAUAAA GGAGAAATT-3′; and shITGB1 #3, 5′-GGAGUUUGCUAAAUUUGAA TT-3′. The target sequences used for shTRAF6 were as follows: 5′- GCAGUGCAAUGGAAUUUAUTT -3' (shTRAF6#1), 5'- GCAAAUGUCAUCUGUGAAUTT -3' (shTRAF6#2) , 5'- CCCAGUCACACAUGAGAAUTT -3' (shTRAF6#3) was used. After transfection for 16 h, the medium was replaced with fresh medium and the transfected cells were selected with 4 μg/mL puromycin for 7 days.

Luciferase reporter assay

To evaluate transactivation activity of NFAT5-TAD, GAL4 reporter gene (PFR-LUC) and GAL4 DNA-binding domain (DBD) -548-1531 containing NFAT5 recombinant TAD were co-transfected into cells. After transfection (24 h), cells were stimulated with EGF and luciferase activity was measured 16 h later using the Luciferase Analysis System Kit (Promega) and the Synergy 2 Multiple Detection Microplate reader (Biotek).

Western blotting and Co-immunoprecipitation (IP) assay

The proteins in the lysate were subjected to sodium dodecyl sulfate (SDS)-polyacrylamide gel electrophoresis, transferred to polyvinylidene fluoride membrane and

blocked in 5% BSA in Tris-buffered saline for 1 h. Membranes were probed with the primary antibodies overnight at 4°C, followed by incubation with secondary antibodies.

To perform IP, cell lysates were incubated with primary antibody overnight at 4°C with gentle shaking, followed by incubation with Protein A/G Sepharose beads (Sigma) for 2 h. Washed the immunoprecipitates with lysis buffer and subjected to immunoblotting analysis.

Immunohistochemical (IHC) staining

Paraffin-embedded tissue sections were baked for 3 h at 60°C and subjected to microwave treatment in citrate buffer for antigen retrieval. Next, the samples were incubated with 3% H_2O_2 for 30 min and blocked with 3% bovine serum albumin (BSA) for 1 h. The sections were incubated with primary antibodies overnight at 4°C, followed incubated with 50μL secondary antibodies (ZSGB-Bio, sp9001) for 30 min. Immunoreactive signals were developed using a 3,3′-diaminobenzidine kit (ZSGB-Bio, China). The sections were counterstained with hematoxylin.

The immunoreactive signal intensity was scored as follows: 0, negative staining; 1, weakly positive staining (light brown); 2, moderately positive staining (brown); and 3, strongly positive staining (dark brown). Additionally, the immunoreactive signals were quantified as follows: 0, negative; 1, positive cells≤ 25%; 2, 26-50% positive cells; 3, 51-75% positive cells; and 4, positive cells > 75%. The EI value, which ranged from 0 to 12, was determined by multiplying the extent (E) and intensity (I) scores.

Detection of apoptosis

Apoptosis was determined using flow cytometry with the phycoerythrin (PE)-conjugated Annexin V/7-aminoactinomycin D (7-AAD) apoptosis detection kit (Beyotime, C1062S). Wash the cells with ice-cold PBS, and resuspend them in Annexin binding buffer, finally reaching a concentration of 106 cells/mL. The cell suspension (100 μL) was incubated with PE-conjugated Annexin V (5 μL) and 7-AAD (5-10 μL) for 15 min in the dark. Add the Annexin binding buffer (400 μL) to the reaction mixture followed by analysis with the flow cytometer (BD FACSVerse).

Promoter activity assay

The human *ITGB1* promoter sequence was downloaded from the USCS genomic browser. The WT and three mutant promoter sequences of *ITGB1* were cloned into the pGL3-basic plasmid and synthesized by Genechem Company (Shanghai, China). The NFAT5-binding sequence was predicted using the HumanTFDB database with the relative threshold set at 80%. The mutant *ITGB1* promoter sequence-harboring vector was constructed using mutated binding sites of NFAT5 at the *ITGB1* promoter region. The WT or mutant *ITGB1* promoter-harboring vector was co-transfected with the control Renilla luciferase reporter into the cells. Luciferase activity was measured by the dual luciferase reporter gene assay system (Promega).

Silver staining and mass spectrometry

The cells were lysed in NETN lysis buffer (50 mM Tris, 0.2 mM EDTA, 1% Triton X-100, 150 mM NaCl, and complete TM protease inhibitor cocktail). Next, the lysates were incubated with anti-FLAG M2 affinity gel (Sigma) with gentle rocking at 4°C for 3 h, followed by incubation with flag-peptides at 4°C for 3 h. To denature the proteins, the samples were incubated at 70°C for 10 min. The bands were visualized using silver staining with a silver staining kit (Pierce, Thermo Fisher). Distinct protein bands were analyzed by LC-MS/MS.

Chromatin immunoprecipitation assay (ChIP)

ChIP analysis was performed using the EZ ChIP Kit (Millipore). The cells were fixed with 1% formaldehyde and neutralized with 0.125 M glycine. Next, the cells were washed with cold PBS three times and lysed in SDS lysis buffer (containing 1% SDS, 50 mM Tris HCl (pH 8.0), and 10 mM EDTA). 200-500-bp chromatin fragments were collected after sonication and pre-cleared in dilution buffer. The fragments were incubated with homologous IgG or NFAT5 antibody on a rotating platform overnight at 4°C. The immunocomplexes were collected using protein G beads and the DNA-binding antibody fragments were eluted for real-time PCR analysis with the following primers: *ITGB1*, 5' -GTCTCACCACCCTTCGTGAC-3' (forward) and 5' -CCTGAGTCCCGAGGCAAATC-3' (reverse).

Animal studies

All animal experiments were approved by the Ethics Committee of the Tianjin Medical University (TMUaMEC2017016). BALB/c nude mice (female, aged 4-5 weeks) were purchased from Viton Lever. The mice were anesthetized (150 μL of 5% chloral hydrate), and 5×10^5 U87/EGFRvIII cells were injected into the frontal lobe of the mouse brain. For drug treatment, mice were intraperitoneally injected with dimethyl sulfoxide (0.3%) or TMZ (60 mg/kg), DZNep (1.5 mg/kg), or TMZ/DZNep combination every other day for 2 weeks. To measure tumor growth, bioluminescence imaging was performed once a week to examine the luciferase activity. The animals were sacrificed and orthotopic tumors were collected for pathological analysis.

Statistical analysis

All experiments were performed in at least triplicates. The data were analyzed using Student's t-test, chi-squared test and Pearson correlation test. All statistical analyses were performed using GraphPad Prism 7.00. *$P < 0.05$; **, $P < 0.01$; ***, $P < 0.001$; and ****, $P < 0.0001$.

Data availability

All remaining data supporting the conclusions of this study are available in the article and supplementary files or from the corresponding authors upon rational request. Source data are provided with the paper.

References

1. Stupp, R. et al. Effects of radiotherapy with concomitant and adjuvant temozolomide versus radiotherapy alone on survival in glioblastoma in a randomised phase III study: 5-year analysis of the EORTC-NCIC trial. *Lancet Oncol.* **10**, 459-466 (2009).
2. Alifieris, C. & Trafalis, D. T. Glioblastoma multiforme: Pathogenesis and treatment. *Pharmacol Ther*. **152**, 63-82 (2015).
3. Stupp, R. et al. Radiotherapy plus concomitant and adjuvant temozolomide for glioblastoma. *N Engl J Med*. **352**, 987-996 (2005).
4. An, Z., Aksoy, O., Zheng, T., Fan, Q. W. & Weiss, W. A. Epidermal growth factor receptor and EGFRvIII in glioblastoma: signaling pathways and targeted therapies. *Oncogene*. **37**, 1561-1575 (2018).
5. Meng, X. et al. Dual functionalized brain-targeting nanoinhibitors restrain temozolomide-resistant glioma via attenuating EGFR and MET signaling pathways. *Nat. Commun.* **11**, 594 (2020).
6. Vengoji, R. et al. Afatinib and Temozolomide combination inhibits tumorigenesis by targeting EGFRvIII-cMet signaling in glioblastoma cells. *J Exp Clin Cancer Res*. **38**, 266 (2019).
7. Lee, J. H. et al. EGFR-Phosphorylated Platelet Isoform of Phosphofructokinase 1 Promotes PI3K Activation. *Mol. Cell.* **70**, 197-210 (2018).
8. Tanaka, K. et al. Oncogenic EGFR signaling activates an mTORC2-NF-kappaB pathway that promotes chemotherapy resistance. *Cancer Discov.* **1**, 524-538 (2011).
9. Weller, M. et al. Rindopepimut with temozolomide for patients with newly diagnosed, EGFRvIII-expressing glioblastoma (ACT IV): a randomised, double-blind, international phase 3 trial. *Lancet Oncol.* **18**, 1373-1385 (2017).
10. Choi, S. Y., Lee-Kwon, W. & Kwon, H. M. The evolving role of TonEBP as an immunometabolic stress protein. *Nat. Rev. Nephrol.* **16**, 352-364 (2020).
11. Miyakawa, H., Woo, S. K., Dahl, S. C., Handler, J. S. & Kwon, H. M. Tonicity-responsive enhancer binding protein, a rel-like protein that stimulates transcription in response to hypertonicity. *Proc Natl Acad Sci U S A*. **96**, 2538-2542 (1999).

12. Chris Y. Cheung et al. Unconventional tonicity-regulated nuclear trafficking of NFAT5 mediated by KPNB1, XPOT and RUVBL2. *bioRxiv*, (2021).
13. Zhang, S. et al. CircFOXO3 promotes glioblastoma progression by acting as a competing endogenous RNA for NFAT5. *Neuro Oncol*. **21**, 1284-1296 (2019).
14. Jiang, Y. et al. Transcription factor NFAT5 contributes to the glycolytic phenotype rewiring and pancreatic cancer progression via transcription of PGK1. *Cell Death Dis.* **10**, 948 (2019).
15. Levy, C. et al. Intronic miR-211 assumes the tumor suppressive function of its host gene in melanoma. *Mol. Cell*. **40**, 841-849 (2010).
16. Jauliac, S. et al. The role of NFAT transcription factors in integrin-mediated carcinoma invasion. *Nat. Cell Biol.* **4**, 540-544 (2002).
17. Janouskova, H. et al. Integrin alpha5beta1 plays a critical role in resistance to temozolomide by interfering with the p53 pathway in high-grade glioma. *Cancer Res.* **72**, 3463-3470 (2012).
18. Lan, Y. et al. Downregulation of SNRPG induces cell cycle arrest and sensitizes human glioblastoma cells to temozolomide by targeting Myc through a p53-dependent signaling pathway. *Cancer Biol Med*. **17**, 112-131 (2020).
19. Huang, K. et al. Genome-Wide CRISPR-Cas9 Screening Identifies NF-kappaB/E2F6 Responsible for EGFRvIII-Associated Temozolomide Resistance in Glioblastoma. *Adv Sci (Weinh)*. **6**, 1900782 (2019).
20. Kim, Y. et al. Methylation-dependent regulation of HIF-1alpha stability restricts retinal and tumour angiogenesis. *Nat. Commun.* **7**, 10347 (2016).
21. Han, D. et al. Lysine methylation of transcription factors in cancer. *Cell Death Dis.* **10**, 290 (2019).
22. Hamamoto, R., Saloura, V. & Nakamura, Y. Critical roles of non-histone protein lysine methylation in human tumorigenesis. *Nat. Rev. Cancer*. **15**, 110-124 (2015).
23. Gunawan, M. et al. The methyltransferase Ezh2 controls cell adhesion and migration through direct methylation of the extranuclear regulatory protein talin. *Nat. Immunol.* **16**, 505-516 (2015).

24. Wang, G. et al. SETDB1-mediated methylation of Akt promotes its K63-linked ubiquitination and activation leading to tumorigenesis. *Nat. Cell Biol.* **21**, 214-225 (2019).
25. Kim, E. et al. Phosphorylation of EZH2 activates STAT3 signaling via STAT3 methylation and promotes tumorigenicity of glioblastoma stem-like cells. *Cancer Cell*. **23**, 839-852 (2013).
26. Fang, L. et al. SET1A-Mediated Mono-Methylation at K342 Regulates YAP Activation by Blocking Its Nuclear Export and Promotes Tumorigenesis. *Cancer Cell*. **34**, 103-118 (2018).
27. Zhu, J., Dou, Z., Sammons, M. A., Levine, A. J. & Berger, S. L. Lysine methylation represses p53 activity in teratocarcinoma cancer cells. *Proc Natl Acad Sci U S A*. **113**, 9822-9827 (2016).
28. Sharifi, Z. et al. Mechanisms and Antitumor Activity of a Binary EGFR/DNA-Targeting Strategy Overcomes Resistance of Glioblastoma Stem Cells to Temozolomide. *Clin. Cancer Res.* **25**, 7594-7608 (2019).
29. Chuikov, S. et al. Regulation of p53 activity through lysine methylation. *Nature*. **432**, 353-360 (2004).
30. Lee, D. Y., Teyssier, C., Strahl, B. D. & Stallcup, M. R. Role of protein methylation in regulation of transcription. *Endocr. Rev.* **26**, 147-170 (2005).
31. Cha, T. L. et al. Akt-mediated phosphorylation of EZH2 suppresses methylation of lysine 27 in histone H3. *Science*. **310**, 306-310 (2005).
32. Chen, X. et al. Melatonin inhibits tumorigenicity of glioblastoma stem-like cells via the AKT-EZH2-STAT3 signaling axis. *J. Pineal Res.* **61**, 208-217 (2016).
33. Kontaki, H. & Talianidis, I. Lysine methylation regulates E2F1-induced cell death. *Mol. Cell*. **39**, 152-160 (2010).
34. Lanouette, S., Mongeon, V., Figeys, D. & Couture, J. F. The functional diversity of protein lysine methylation. *Mol. Syst. Biol.* **10**, 724 (2014).
35. Williams, R. L. & Urbe, S. The emerging shape of the ESCRT machinery. *Nat Rev Mol Cell Biol*. **8**, 355-368 (2007).

36. Zhang, X. et al. TRAF6 Restricts p53 Mitochondrial Translocation, Apoptosis, and Tumor Suppression. *Mol. Cell*. **64**, 803-814 (2016).
37. Meng, Y. et al. TRAF6 mediates human DNA2 polyubiquitination and nuclear localization to maintain nuclear genome integrity. *Nucleic Acids Res.* **47**, 7564-7579 (2019).
38. Lee, N., Kim, D. & Kim, W. U. Role of NFAT5 in the Immune System and Pathogenesis of Autoimmune Diseases. *Front Immunol*. **10**, 270 (2019).
39. Wei, J. et al. Osteopontin mediates glioblastoma-associated macrophage infiltration and is a potential therapeutic target. *J. Clin. Invest.* **129**, 137-149 (2019).
40. Liu, Y. et al. Rolling-translated EGFR variants sustain EGFR signaling and promote glioblastoma tumorigenicity. *Neuro Oncol*. **23**, 743-756 (2021).
41. Oldrini, B. et al. MGMT genomic rearrangements contribute to chemotherapy resistance in gliomas. *Nat. Commun.* **11**, 3883 (2020).
42. Wu, S. et al. PARP-mediated PARylation of MGMT is critical to promote repair of temozolomide-induced O6-methylguanine DNA damage in glioblastoma. *Neuro Oncol*. **23**, 920-931 (2021).
43. Varambally, S. et al. The polycomb group protein EZH2 is involved in progression of prostate cancer. *Nature*. **419**, 624-629 (2002).
44. Caretti, G., Di Padova, M., Micales, B., Lyons, G. E. & Sartorelli, V. The Polycomb Ezh2 methyltransferase regulates muscle gene expression and skeletal muscle differentiation. *Genes Dev*. **18**, 2627-2638 (2004).
45. Wu, Y. et al. Tamoxifen Resistance in Breast Cancer Is Regulated by the EZH2-ERalpha-GREB1 Transcriptional Axis. *Cancer Res.* **78**, 671-684 (2018).
46. Bao, Y. et al. EZH2-mediated PP2A inactivation confers resistance to HER2-targeted breast cancer therapy. *Nat. Commun.* **11**, 5878 (2020).
47. Zhang, Z. et al. PLK4 is a determinant of temozolomide sensitivity through phosphorylation of IKBKE in glioblastoma. *Cancer Lett.* **443**, 91-107 (2019).

Figure Legends

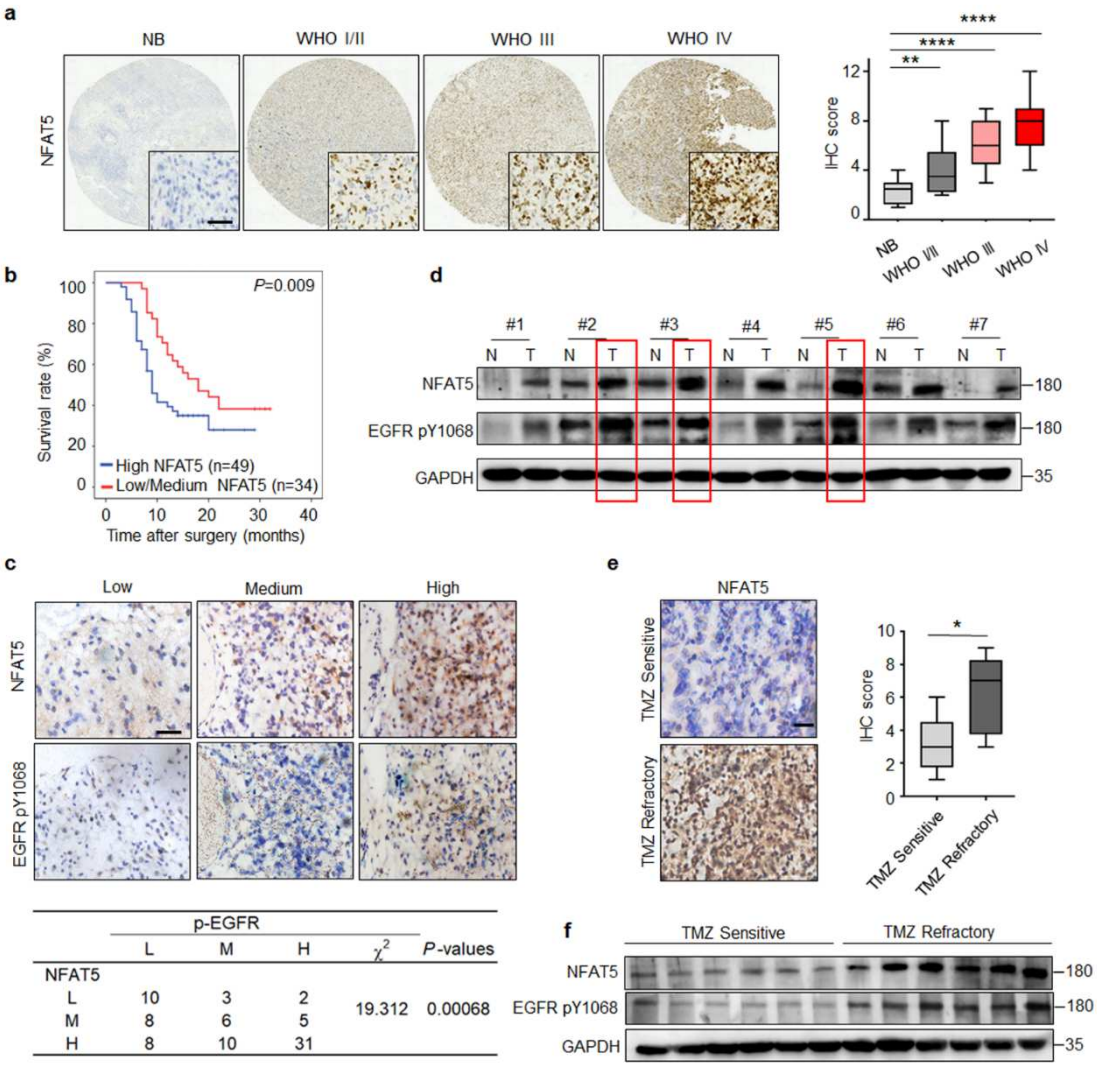

	p-EGFR				
NFAT5	L	M	H	χ^2	*P*-values
L	10	3	2	19.312	0.00068
M	8	6	5		
H	8	10	31		

Figure. 1. NFAT5 expression is upregulated in TMZ-resistant GBM specimens and positively correlates with p-EGFR expression.

a, Representative immunohistochemical (IHC) staining of NFAT5 in tumorous and adjacent non-tumorous brain (NB) tissues (left) of patients with glioma (NB: 8 cases; WHO I/II: 12 cases; WHO III: 16 cases; WHO IV: 55 cases). Scale bar: 100μm. IHC analysis of NFAT5 expression at different tumor stages (right). $^{**}P < 0.01$, $^{****}P < 0.0001$. **b,** Kaplan-Meier survival analysis of patients with glioma (log-rank tests). The overall survival of patients with low/medium NFAT5 expression was lower than that of patients with high NFAT5 expression. **c,** Upper, NFAT5 and EGFR pY1068 expression in glioma tissues determine by IHC staining. Bottom, IHC staining of NFAT5 and EGFR pY1068 expression in 83

691 human glioma samples statistically analyzed using chi-squared tests. Scale bar: 100μm**.**
692 **d,** The NFAT5 and EGFR pY1068 levels in clinical GBM samples and paired adjacent non-
693 tumorous tissue. N, normal; T, tumor. **e,** Representative IHC staining of NFAT5 in TMZ
694 sensitive and resistant GBM tissues. Scale bar: 100μm**.** *$P < 0.05$. **f,** The expression of
695 NFAT5 and EGFR pY1068 in the TMZ sensitive and refractory GBM specimen.

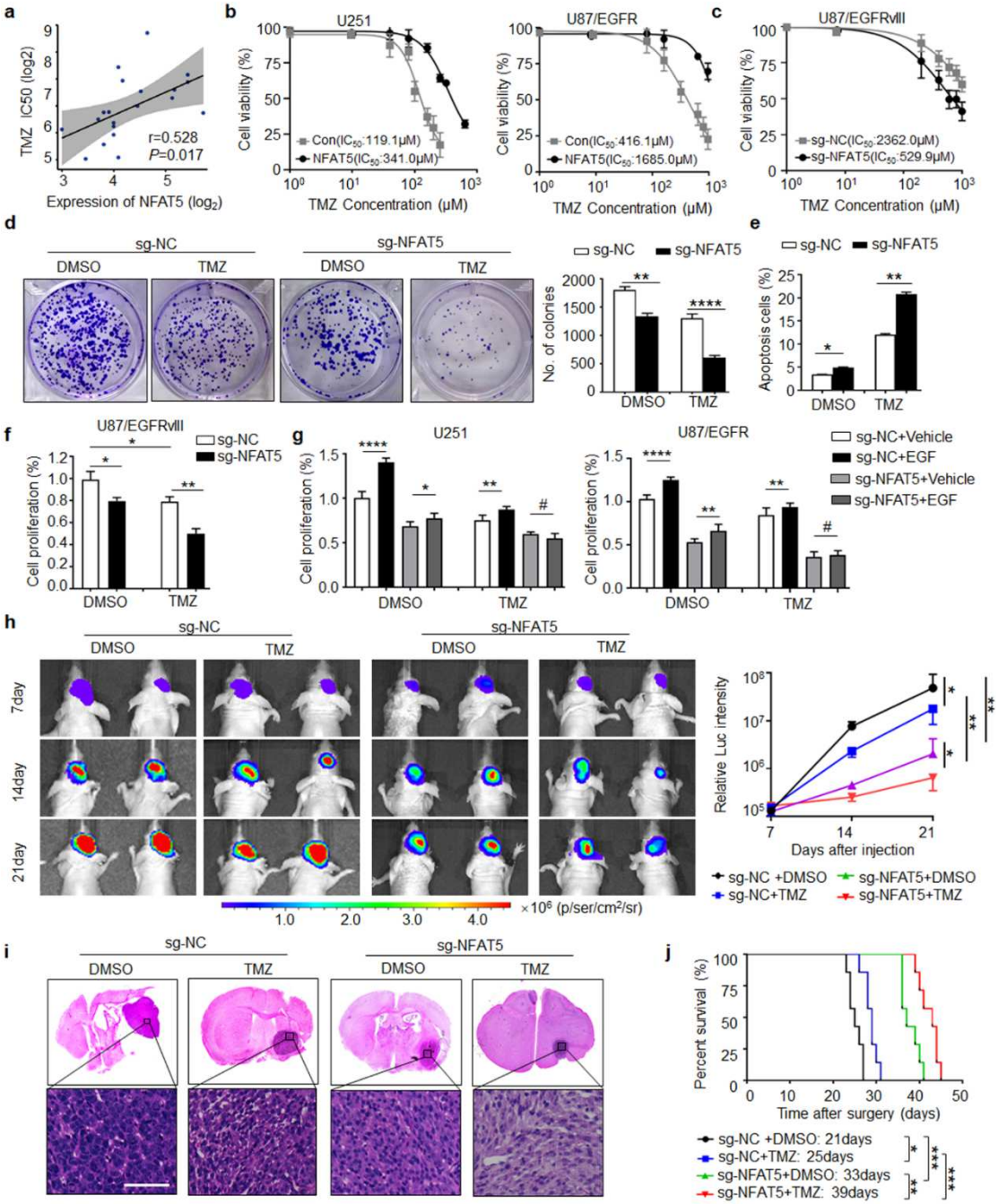

Figure. 2. NFAT5 drives EGFR activation induced tumor growth and the failure of TMZ therapy.

a, The association between NFAT5 expression and TMZ response from 20 GBM cell lines from the Genomics of Drug Sensitivity in Cancer (GDSC) database. **b-c,** The effect of NFAT5 on TMZ efficacy at the indicated concentrations determined by CCK-8 assay (n = 5). **d,** Colony formation assay in U87/EGFRvIII cells expressing sg-NC or sg-NFAT5 with or without TMZ treatment (200μM). $^{**}P < 0.01$, $^{****}P < 0.0001$. **e,** Flow cytometry analysis

of the effect of NFAT5 knockout on the percentage of apoptotic cells in U87/EGFRvIII cells with or without TMZ treatment (200μM, 72h). *P < 0.05; **P < 0.01. **f,** Knockout of NFAT5 induced cell proliferation and TMZ refractory (200μM, 72h) in U87/EGFRvIII cells. *P < 0.05; **P < 0.01. **g,** Loss of NFAT5 attenuated EGFR activation induced cell proliferation and TMZ refractory (200μM, 72h) in U251 and U87/EGFR cells. *P < 0.05; **P < 0.01; ****P < 0.0001; $^{\#}$Not significant. **h,** Representative bioluminescence images of Balb/c nude mice with tumors derived from U87/EGFRvIII cells transfected with sg-NC or sg-NFAT5 treated with TMZ every week (n = 7 mice/group). *P < 0.05; **P < 0.01. **i,** H&E stained coronal brain sections of representative tumor xenograft. Scale bar: 100μm. **j,** Survival of mice bearing U87/EGFRvIII tumors shown in (h).*P < 0.05; **P < 0.01; ***P < 0.001.

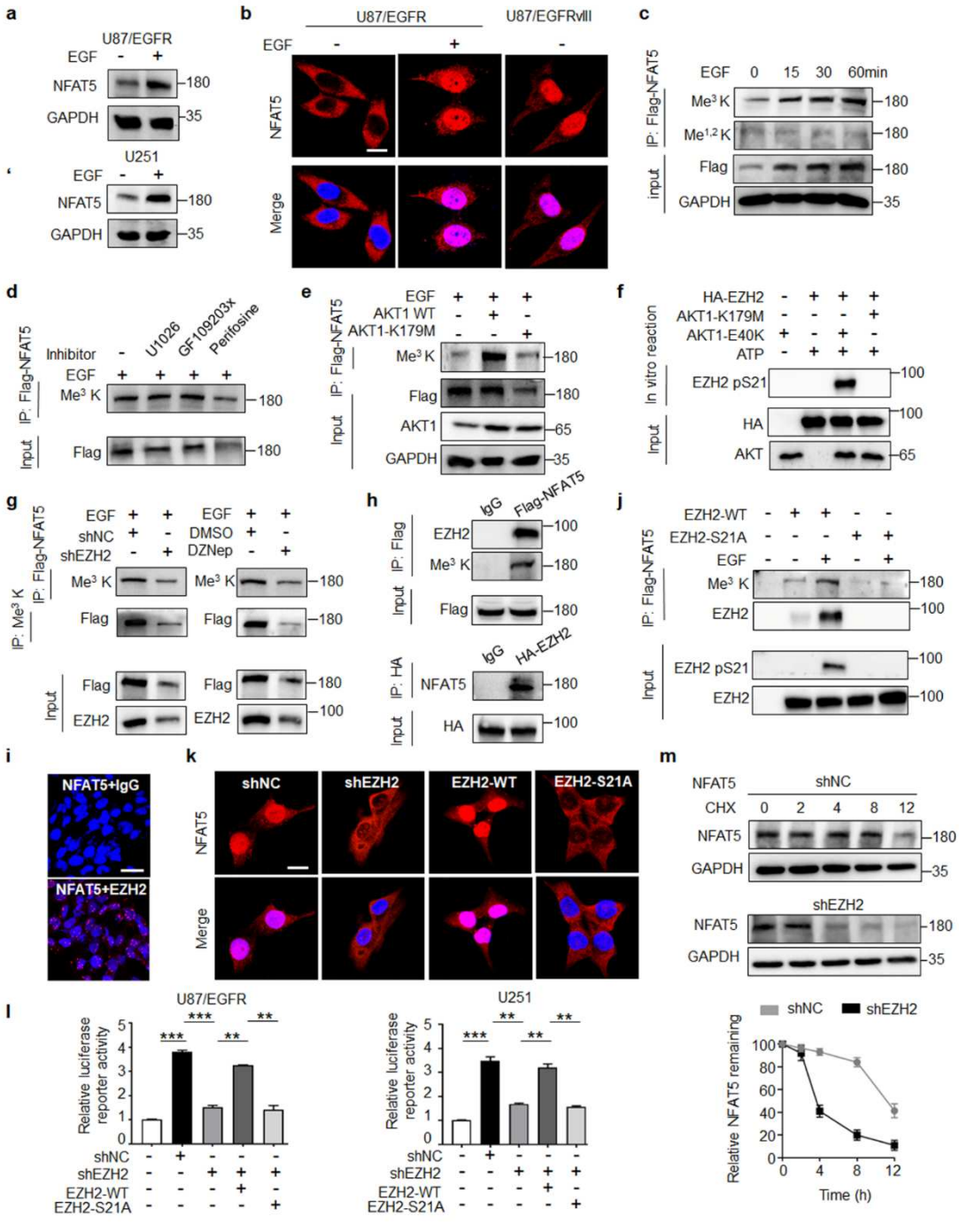

Figure. 3. EGF induces NFAT5 lysine methylation and activation dependent on EZH2. **a,** NFAT5 protein levels in U87/EGFR and U251 cells upon EGF stimulation. **b,** Immunofluorescence staining shown the subcellular location of NFAT5 in U87/EGFRvIII cells and U87/EGFR cells with or without EGF treatment. Scale bar: 20μm. **c,** The effect of different incubation times of EGF treatment on the expression and lysine methylation levels of NFAT5. **d,** Levels of NFAT5 lysine methylation in U87/EGFR cells incubated with 10 μM PKCα (GF109203X), 10 μM MEK1 (U0126), or 10 μM AKT1 (perifosine) inhibitors for 24 h

followed by EGF (100 ng/ml) for 15min. **e,** AKT1 kinase activity was required for EGF induced NFAT5 tri-lysine methylation. U251 cells transduced with lentiviral vectors harboring Flag-tagged kinase-dead mutant AKT-K179M or AKT-WT sequences. **f,** In vitro kinase assay revealed that AKT1-mediated EZH2 phosphorylation at Ser21 in U251 cells. **g,** Knockdown of EZH2 by shRNA or a small molecule inhibitor (DZNep) treatment reduced NFAT5 lysine methylation induced by EGF stimulation in U87/EGFR cells. **h,** Co-immunoprecipitation assay was performed to examine EZH2 as an interactor of NFAT5 in the U251 cells. **i,** The results of the in situ proximity ligation assay revealed the direct interaction between NFAT5 and EZH2 in U251 cells. Scale bar: 100μm. **j,** EZH2 phosphorylation at Ser21 was critical for EZH2/NFAT5 interaction and NFAT5 methylation upon EGF stimulation. **k,** Immunofluorescence staining shown the subcellular location of NFAT5 transfected with shNC, shEZH2, EZH2-WT and EZH2-S21A in U251 cells treated with EGF. Scale bar: 20μm. **l,** NFAT5 TAD reporter luciferase activity was measured in cells transfection with shEZH2, EZH2-WT, EZH2-S21A and EZH2-S21D cells upon EGF treatment in U87EGFR and U251 cell. $^{**}P < 0.01$; $^{***}P < 0.001$. **m,** Degradation of NFAT5 was assessed by CHX treatment transfected with shNC or shEZH2 in U251 cell. Below, quantification of the NFAT5 intensity.

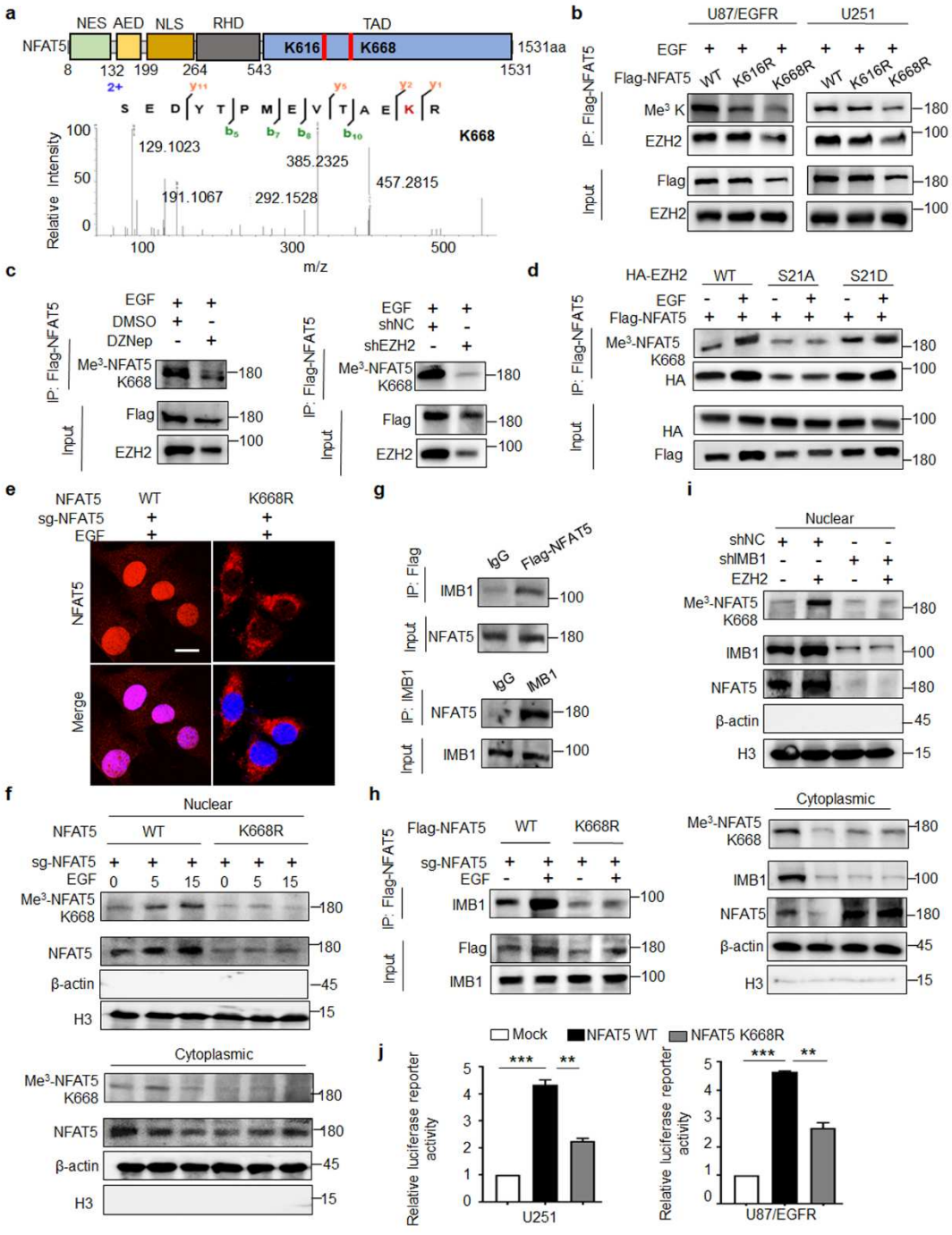

739

740 **Figure. 4. Methylation at K668 determines NFAT5 nuclear localization and activation**

741 **a.** Identification of lysine methylation site of NFAT5 by LC-MS/MS, corresponding to one of

742 two methylation sites, K668. **b,** K668 (but not K616) mitigated EGF-induced NFAT5 tri-

743 methylation and EZH2/NFAT5 interaction. **c,** Knockdown EZH2 by shRNA or DZNep

744 mitigated EGF-induced NFAT5 K668 methylation in U87/EGFR cells. **d,** Expression of Me^3-

745 NFAT5 K668 and the association between NFAT5 and EZH2 was analyzed in HA-tagged

EZH2 WT, S21A, S21D expressing U251 cells. **e,** Immunofluorescence staining of NFAT5 expression in U251 cells stably expressing NFAT5 WT or K668R mutant. Scale bar: 20μm**.** **f,** The nuclear and cytosolic fractions of U87/EGFR cells expressing NFAT5 WT or K668R mutant treated with EGF at different times were subjected to immunoblotting analysis. **g,** Co-IP assay was performed to examine IMB1 as an interactor of NFAT5 in the U251 cells. **h,** The association of NFAT5 and IMB1 was examined in NFAT5 WT or K668R cells in the presence of EGF or not. **i,** The nuclear and cytosolic expression of NFAT5 and Me^3-NFAT5 K668 was detected in EZH2 overexpressing cells transfected with shNC or shIMB1. **j,** NFAT5 TAD reporter luciferase activity was measured in cells transfected with NFAT5 WT or K668R. $^{**}P < 0.01$; $^{***}P < 0.001$.

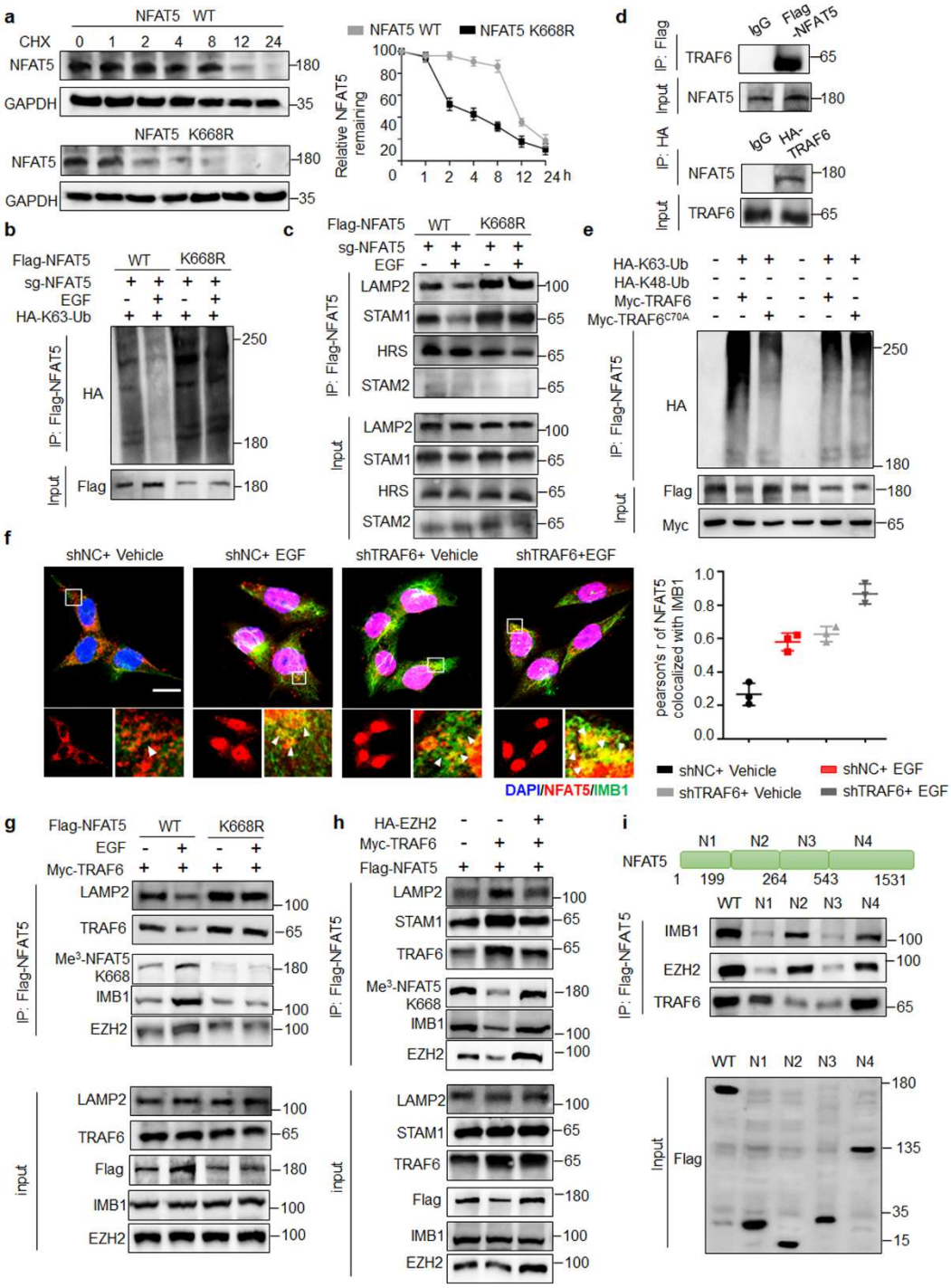

Figure. 5. Methylation protects NFAT5 from ubiquitin-mediated lysosome degradation and cytosol restriction by attenuating its binding to E3 ligase TRAF6. **a,** Degradation of NFAT5 was assessed by CHX treatment in NFAT5 WT or K668R mutant expressing U251 cells. Right, quantification of the NFAT5 intensity. **b,** NFAT5 K63-linked ubiquitination and the association between NFAT5 and ESCRT-0 complex (**c**) were examined in U251 expressing NFAT5 WT and K668R mutant cells. **d,** Co-IP analysis of the

763 interaction between TRAF6 and NFAT5 in U251 cells. **e,** TRAF6 activation was required
764 for NFAT5 K63 but not K48-linked ubiquitination. **f,** Immunofluorescence staining of NFAT5
765 nuclear distribution and co-localization between NFAT5 and IMB1 in shNC or shTRAF6
766 transfected U251 cells in the presence of EGF or not. **g,** The interaction between NFAT5
767 and TRAF6, EZH2, LAMP2 as well as IMB1 was examined in TRAF6 overexpressing cells
768 in the absence or presence of EGF stimulation. **h,** The association of NFAT5 with TRAF6,
769 EZH2, LAMP2, STAM1 as well as IMB1 was examined in TRAF6 overexpressing cells in
770 the absence or presence EZH2 transfection. **i,** Identification of the essential domains
771 required for interactions of NFAT5 with TRAF6, EZH2 and IMB1. Diagrammatic
772 representation of NFAT5 and its truncated forms.

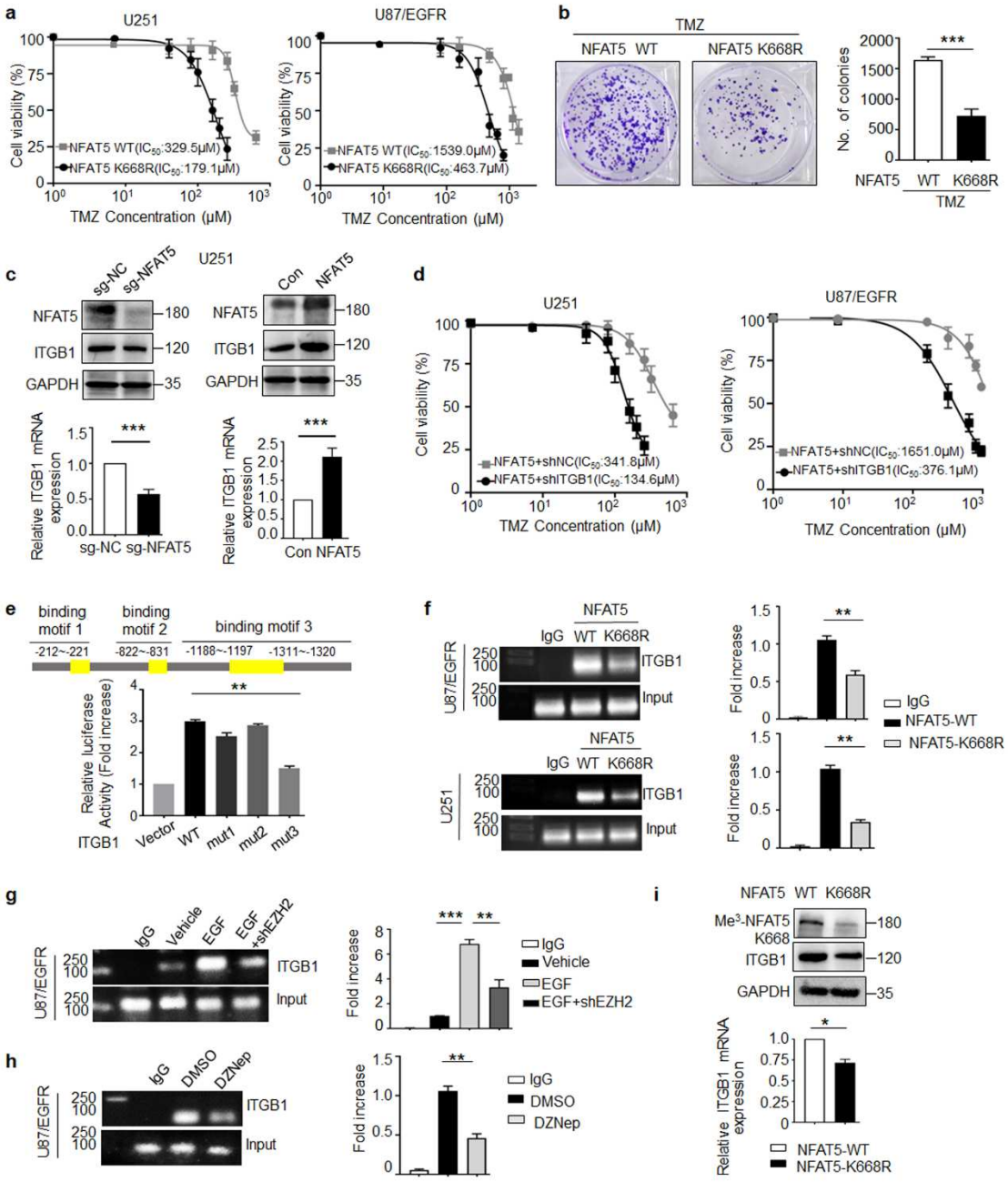

773

774 **Figure. 6. K668 methylation is required for NFAT5 induced limited TMZ efficacy by**

775 **enhanced *ITGB1* transcription.**

776 **a,** CCK-8 assay analysis revealed the effect of NFAT5 K668 methylation on TMZ treatment

777 efficacy at the indicated concentrations for 72 h (n=5). **b,** Colony formation assay in

778 U87/EGFRVIII cells expressing NFAT5 WT or K668R with TMZ treatment. ****P* < 0.001. **c,**

779 The effect of NFAT5 on ITGB1 protein expression and mRNA levels in U251 cells. ****P* <

780 0.001. **d,** The results of the CCK-8 assay revealed the effect of ITGB1 knockdown on TMZ

781 treatment efficacy (at the indicated concentrations) in NFAT5-overexpressing U87/EGFR

and U251 cells (n = 5). **e,** The results of the dual-luciferase reporter assay revealed that ITGB1 was a direct transcriptional target of NFAT5. $^{**}P < 0.01$. **f,** ChIP assays shown that NFAT5 K668R mutation reduced NFAT5 binding affinity to *ITGB1* promoter, compare to the NFAT5 WT cells. $^{**}P < 0.01$. **g,** CHIP assay revealed that *EZH2* knockdown by shRNA or DZNep treatment **(h)** decreased the binding affinity of NFAT5 to the promoter of *ITGB1* in U87/EGFR cells. $^{**}P < 0.01$; $^{***}P < 0.001$. **i,** The protein and mRNA levels of ITGB1 in U87/EGFR cells expressing NFAT5 WT or K668R mutation. $^{**}P < 0.01$.

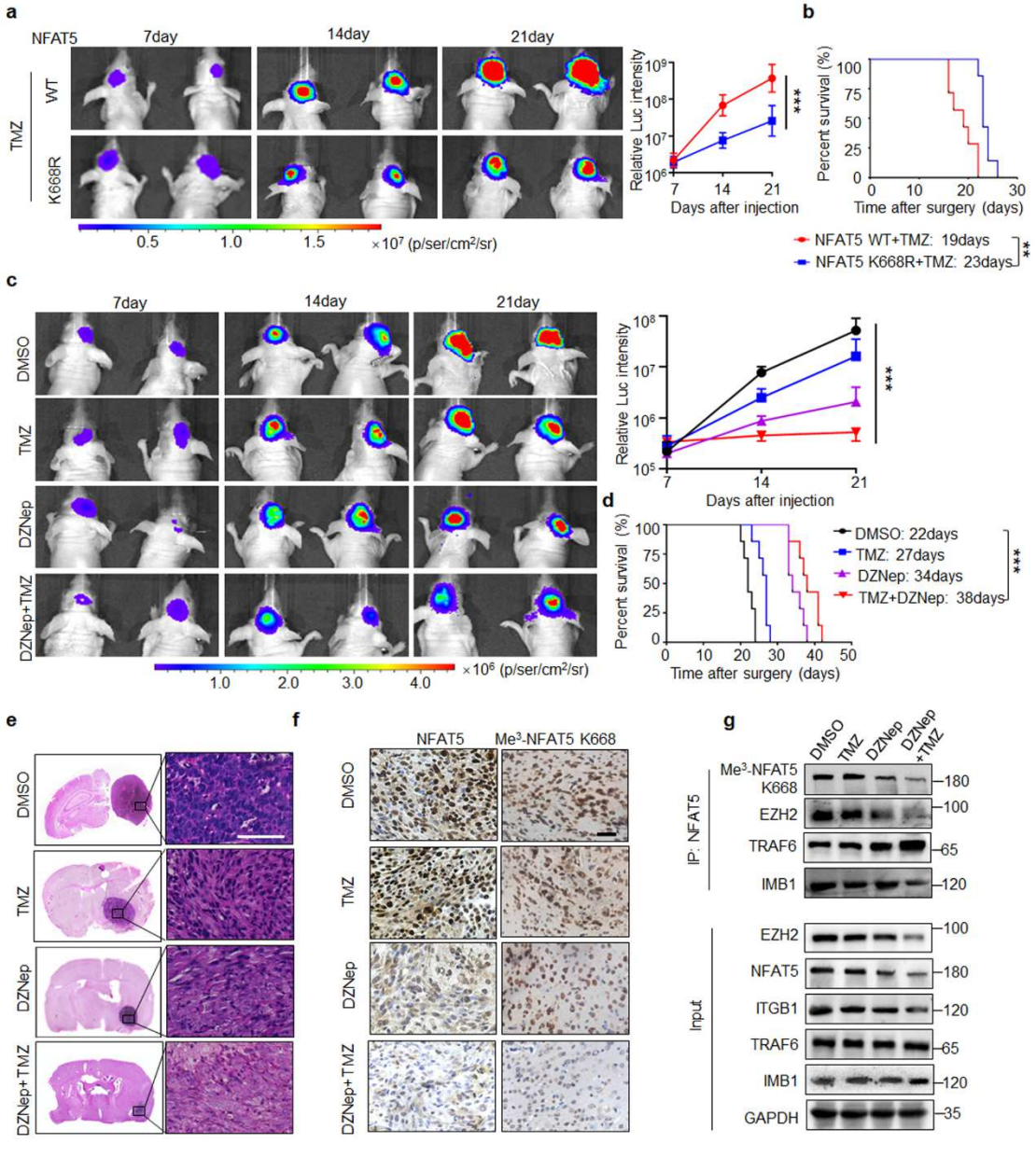

Figure. 7. Inhibition of NFAT5 K668 methylation improves TMZ efficacy in vivo.

A, Representative bioluminescent images of Balb/c nude mice harboring tumors derived from NFAT5 WT or K668R mutant-transfected U87/EGFRvIII cells treated with TMZ therapy every week. Right, Tumor burden examined by bioluminescence imaging (n = 7 mice/group). ***P < 0.001. **b,** Kaplan-Meier survival curves of mice shown in (a). **P < 0.01. **c,** Effects of TMZ, DZNep, alone or in combination on tumor growth in mice harboring U87/EGFRvIII cell-derived tumors. Right, Tumor burden examined by bioluminescence imaging (n = 7 mice/group). ***P < 0.001. **d,** Survival of mice injected with TMZ, DZNep alone or in combination. ***P < 0.001. **e,** H&E-stained coronal brain sections of mice from

799 experiment shown in (c). Scale bar: 100μm. **f,** IHC staining of NFAT5 and Me^3-NFAT5 K668
800 expression in the tumors from each group. **g,** Combination of TMZ and DZNep impaired
801 the interaction between NFAT5 and EZH2 as well as IMB1 in mice.

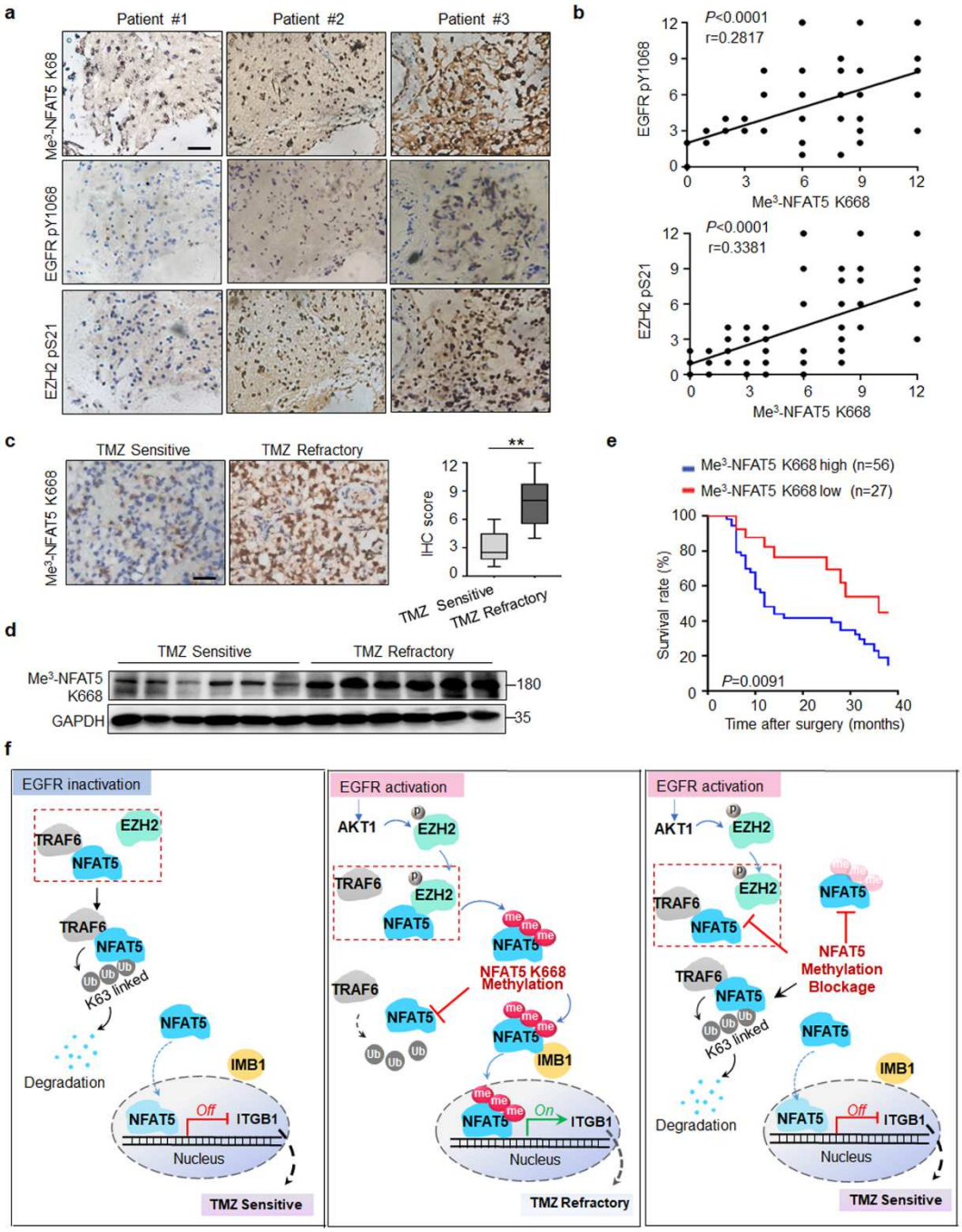

Figure. 8. NFAT5 K668 methylation is positively correlated with EGFR pY1068 and EZH2 pS21 expression, TMZ refractory and poor prognosis in patients with GBM. **a,** IHC staining of Me^3-NFAT5 K668, EZH2 pS21 and EGFR pY1068 expression in 83 glioma specimens. Scale bar: 100μm. **b,** IHC stains were scored and the correlation was carried out by Pearson correlation test. **c,** Representative IHC-staining of Me^3-NFAT5 K668 in TMZ-sensitive and resistant GBM tissues. Scale bar: 100μm. $^{**}P < 0.01$. **d,** Protein expression of Me^3-NFAT5 K668 in TMZ sensitive and resistant clinical GBM samples. **e,**

Kaplan-Meier survival analysis of patients (log-rank tests). Overall survival of patients with high Me^3-NFAT5 K668 expression was shorter. **f,** A proposed model illustrating lysine methylation of NFAT5 drives tumor progression and TMZ refractoriness in GBM. NFAT5 undergoes K668 methylation by EZH2 upon EGF stimulation, resulting in NFAT5 nuclear translocation and activation. Methylation disrupts NFAT5 binding to E3 ligase TRAF6, which is crucial for NFAT5 K63-linked ubiquitination mediated lysosomal degradation and cytosol localization restriction, leading to NFAT5 stabilization, nuclear accumulation and activation. Nuclear NFAT5 increased the induction of ITGB1, a transcriptional target of NFAT5, which is required for unfavorable TMZ response. This suggests the development of new strategies involving NFAT5 K668 methylation blockage for enhancing TMZ response in GBM.

Supplementary Files

This is a list of supplementary files associated with this preprint. Click to download.

- SupplementaryMaterials.pdf